

Modelling of multi-connected acoustical spaces by the surface impedance approach

Goran PAVIC¹; Liangfen DU²

LVA, INSA Lyon, France

ABSTRACT

The acoustical surface impedance has been conceived as a tool of modelling sound transmission or of characterising air-borne noise sources. The same technique can be alternatively used to model acoustical properties of multi-connected acoustical spaces. This approach is particularly advantageous where an analytical model of each individual space is available. Two surface impedance techniques are presented: the patch technique and the surface harmonics technique. The advantages and disadvantages of the two techniques are discussed. Modelling examples of multi-connected rooms are shown which demonstrate the validity and the potential of this approach.

Keywords: Sound, Modelling, Closed space I-INCE Classification of Subjects Numbers: 25.2, 75.9

1. INTRODUCTION

The usual way to model sound in a cavity is by means of simple statistical Eyring-Sabine theory (1). This gives space- and frequency-averaged value of sound pressure. In cases where more detailed modelling is required the statistical approach is replaced by numerical field discretization techniques: FEM or BEM. The numerical techniques require the use of specialized software while the results are limited to primary field variables: sound pressure and particle velocity. In a number of applications the use of analytical models may be advantageous.

The analytical modelling of sound field in a closed cavity is limited to some basic simple shapes, such as a sphere, a cylinder or a parallelepiped. The modelling is based on the field decomposition in eigenfunctions of the space concerned. If the entire acoustical space considered can be broken down to a number of simple spaces, the eigenfunctions of which are known, the acoustics of the global space can be potentially modelled by substructuring using the coupling continuity conditions.

A particular interest for use of modal methods was shown for duct-type cylindrical cavities. E.g. in (2) the authors have worked out analytical eigenmode solutions for hollow and annular elliptical cavities. To provide for the coupling between substructures the mode matching method has been mostly applied, e.g. in the acoustic analysis of mufflers (3).

In this paper a simple engineering approach based on surface coupling between acoustic spaces will be investigated. The approach focuses on the modelling of acoustical cavities composed of several sub-cavities of simple shape.

2. COUPLING OF TWO UNEQUAL CAVITIES USING PATCH APPROACH

The objective of this section is to focus on some basic features of multi-space coupling. This will be done using patch coupling technique (1). This technique allows for continuous surface coupling of acoustical spaces by discrete patch approximations. Analytical modelling will be applied using the Green's function obtained by classical modal superposition. The analysis is done in frequency domain which allows the use of complex amplitudes and the suppression of time-dependent terms.

2.1 The Acoustical Space

To demonstrate the multi-space coupling technique in a simple way an ordinary parallelepipedic volume is used as a global acoustical space. The entire volume is divided by a fictitious surface $S =$

¹ goran.pavic@insa-lyon.fr

² liangfen.du@insa-lyon.fr

$S_1 \cup S_2$ into two cavities: a simple cavity Ω_s , containing a monopole source and an L-shaped cavity Ω_r , which acts as a receiver space, Fig. 1. The two cavities will be modelled separately and then coupled together to obtain response in the receiver cavity. The response in a point A , chosen at random at $[0.7292, 0.1409, 0.1464]$ m, will serve to compare the sound pressure computed directly and by coupling of the two sub-cavities.

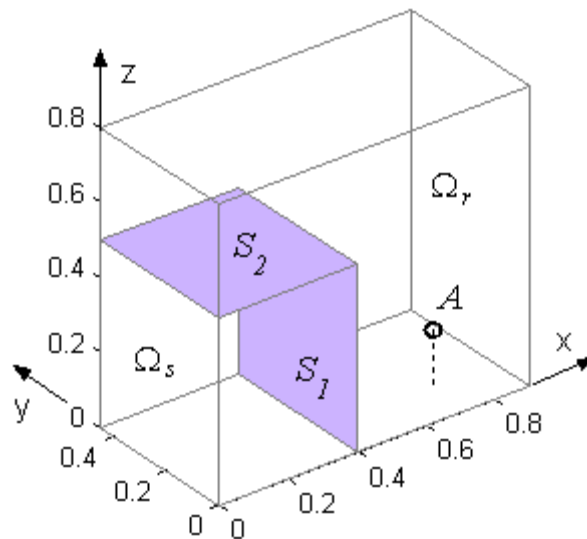


Figure 1 – Acoustical space and its subspaces

The analysis will be done in the 500 Hz octave band, i.e. spanning from 354Hz to 707 Hz. The wavelength affects the patch spatial averaging and thus its optimum size. One octave band was considered to be a good compromise between the need to have wide enough frequency coverage and yet narrow enough width which can be easily associated to a representative single frequency: the band centre frequency. To this end any octave band could have been chosen, however the 500 Hz band was believed to be well representative of typical noise problems.

It is known that a very large number of modes need to be taken into account where patch coupling is concerned. In the present paper the solution is found analytically, thus a very large number of modes could be used. In this way the convergence of the solution with the increase of number of modes could be monitored. In the current case all the modes having the natural frequencies up to 20 kHz, were included in the computation. This corresponds to some 277,000 modes for the entire system. Such a large number is not needed where direct computation of sound pressure is concerned, but is needed with the patch coupling approach.

2.2 Impedance and response of an L-shaped cavity

In this section, an analytical solution is given for the patch impedances of an L-shaped cavity. Such a solution will be itself obtained by again using the patch coupling approach. The L-shaped space will be divided into two simple parallelepipedic cavities, coupled by the surface S_c , Fig. 2, left.

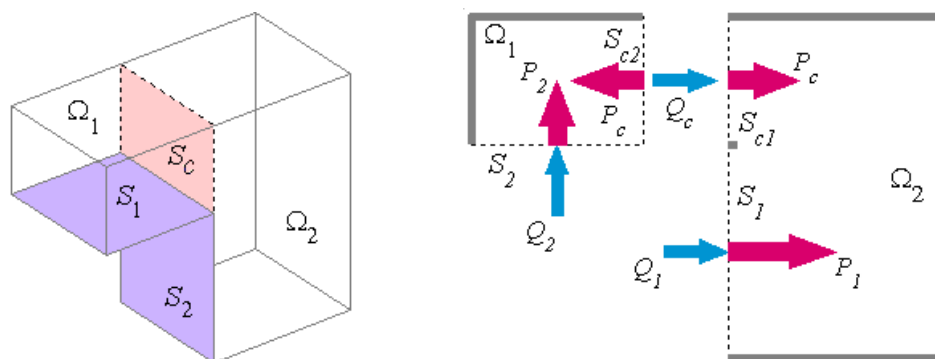


Figure 2 – Modelling of impedance of an L-shaped cavity

The continuity conditions at different interfaces give 4 matrix equations, Fig. 2 right:

$$\begin{aligned} P_1 &= Z_{1,1} Q_1 + Z_{1,c1} Q_c \\ P_2 &= Z_{2,2} Q_2 - Z_{2,c2} Q_c \\ P_c &= Z_{c1,1} Q_1 + Z_{c1,c1} Q_c = Z_{c2,2} Q_2 - Z_{c2,c2} Q_c \end{aligned} \quad (1)$$

Here P stand for the vectors of mean patch pressure amplitudes, Q are the vectors of driving patch volume velocity amplitudes and Z are the impedance matrices linking the two. In order to distinguish between interface variables belonging to cavities 1 and 2, the subscripts $c1$ and $c2$ are used. E.g. the symbol $Z_{c1,1}$ denotes the transfer matrix between the response patches at S_{c1} and the driving patches at S_1 . The solution for sound pressure vectors to the system of equations (1) reads:

$$\begin{aligned} P &= Z Q, \quad P = \begin{Bmatrix} P_1 \\ P_2 \end{Bmatrix}, \quad Q = \begin{Bmatrix} Q_1 \\ Q_2 \end{Bmatrix} \\ Z &= \begin{bmatrix} (Z_{1,1} - Z_{1,c1} M_c Z_{c1,1}) & Z_{1,c1} M_c Z_{c2,2} \\ Z_{2,c2} M_c Z_{c1,1} & (Z_{2,2} - Z_{2,c2} M_c Z_{c2,2}) \end{bmatrix} \\ M_c &= (Z_{c1,c1} + Z_{c2,c2})^{-1} \end{aligned} \quad (2)$$

The matrix Z , consisting of 4 sub-matrices, clearly represents the impedance matrix of the coupling surface S . The matrix M_c physically represents the mobility of the two coupled cavities blocked at S and driven via the interface surface S_c . The impedance Z given by (2), which in the present case refers to the receiver, $Z_r = Z$, is needed for global sub-structuring with the goal of finding the acoustical state at the source-receiver interface. Once this state has been identified, each cavity can be treated locally, by imposing the coupling velocities, either Q_1 and Q_c or Q_2 and Q_c , at the interface surface S .

The velocity vector Q_c is an internal coupling variable which yet needs to be found. Depending on whether the reception points A within the receiver falls in the section Ω_1 or Ω_2 , the equations for the pressure vector P_A take in the present case the following form:

$$\begin{aligned} P_A &= Z_{A,1} Q_1 + Z_{A,c1} Q_{c1} \quad A \in \Omega_1 \\ P_A &= Z_{A,2} Q_2 + Z_{A,c2} Q_{c2} \quad A \in \Omega_2 \end{aligned} \quad (3)$$

Together with Eqs. (2) the system above yields the solution for P_A as a function of external coupling volume velocity vectors Q_1 and Q_2 :

$$\begin{aligned} P_A &= \begin{bmatrix} (Z_{A,1} - Z_{A,c1} M_c Z_{c1,1}) & 0 \\ 0 & (Z_{A,c1} M_c Z_{c2,2}) \end{bmatrix} \begin{bmatrix} Q_1 \\ Q_2 \end{bmatrix} \quad A \in \Omega_1 \\ P_A &= \begin{bmatrix} (Z_{A,c2} M_c Z_{c1,1}) & 0 \\ 0 & (Z_{A,2} - Z_{A,c2} M_c Z_{c2,2}) \end{bmatrix} \begin{bmatrix} Q_1 \\ Q_2 \end{bmatrix} \quad A \in \Omega_2 \end{aligned} \quad (4)$$

2.3 Variation of parameters

In this section a variation is made of two key parameters of patch coupling modelling: the patch size and the number of modes taken into account. The second parameter will matter only if the sound pressure is treated by computation; any measured data will be sensitive to the first parameter only.

The term patch size means here the average patch linear dimension. To start with, a particular patch linear dimension is defined as a fraction of mean wavelength (equal to $343/500 = 0.686\text{m}$). Each of the coupling areas, S_1 , S_2 and S_c , is then subdivided into equal patches which fit the best this value. Five values of patch size / wavelength ratio ζ were analysed: 0.15, 0.2, 0.3, 0.4 and 0.6. In this way, five patch patterns were obtained for each coupling surface. The number of patches per surface in two directions is shown in Table 1.

For each patch configuration the number of modes was varied eight times in steps of $\sqrt{10}$: 100, 316,

1,000....316,000. In terms of natural frequencies of the entire volume considered, these values correspond to the highest natural frequencies of 1.22, 1.92, 2.90, 4.35, 6.48, 9.58, 14.2 and 20.9 kHz respectively. To provide sound excitation two monopoles of complex amplitudes $Q_1 = 1 \times 10^{-3} \text{ m}^3/\text{s}$ and $Q_2 = 2j \times 10^{-3} \text{ m}^3/\text{s}$ were placed at two points chosen at random: [0.1176, 0.2682, 0.3860] and [0.2352, 0.1616, 0.0740] m respectively.

Table 1 – Number of patches per coupling surface

| ζ | 0.15 | 0.2 | 0.3 | 0.4 | 0.6 |
|-------------------------------|--------------|--------------|--------------|--------------|--------------|
| S_1 , width \times height | 4 \times 5 | 3 \times 3 | 2 \times 2 | 2 \times 2 | 1 \times 1 |
| S_2 , length \times width | 4 \times 4 | 3 \times 3 | 2 \times 2 | 1 \times 2 | 1 \times 1 |
| S_c , width \times height | 4 \times 3 | 3 \times 2 | 2 \times 2 | 2 \times 1 | 1 \times 1 |

Fig. 3 compares the solutions obtained by patch coupling and directly for two cases. The case on the left has the theoretical ratio between the average patch size and the wavelength $\zeta = 0.3$, which corresponds to 4 patches per each surface, Table 2. The number of modes used was 10,000. On the right is shown the case of $\zeta = 0.15$, i.e. 48 patches in total, using 316,000 modes.

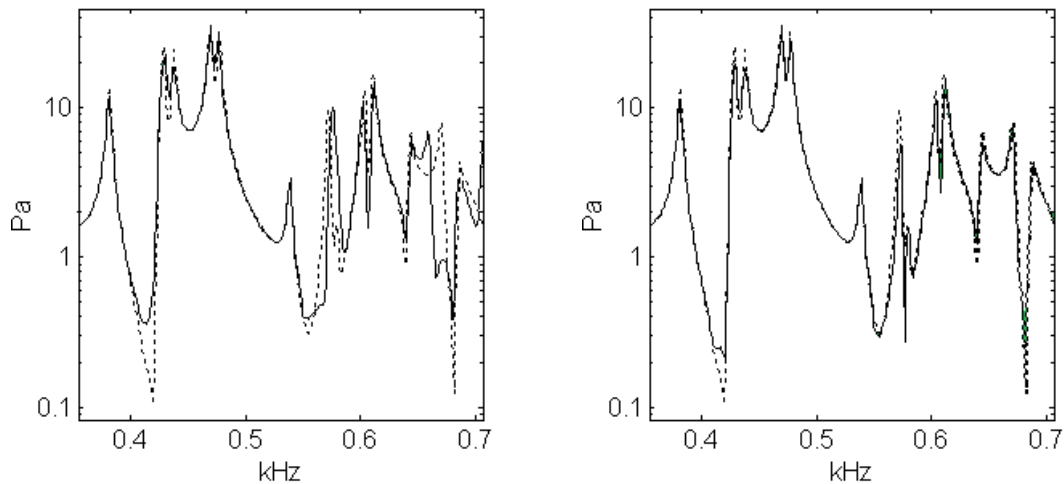


Figure 3 – Sound pressure response by patch coupling (full line) and direct solution (dotted line). Left: mean patch size / mean wavelength = 0.3; 10,000 modes. Right: mean patch size / mean wavelength = 0.15; 316,000 modes.

As expected, using the smallest patches and the highest number of modes results in a very good matching with the exact solution. The other case, that of moderate patch size and a relatively low number of modes used, gives a result which is acceptable in a global sense, but which shows some considerable mismatch at individual frequencies, especially in the upper half of the band analysed.

In order to better apprehend the influence of the two parameters on the accuracy of results, a simultaneous comparison will be made of all the $5 \times 8 = 40$ cases analysed. The matching between the patch coupling solution P and the exact solution P_0 will be expressed for each case by a single value, the cumulative relative error, defined as:

$$e_c = \frac{1}{f_2 - f_1} \int_{f_1}^{f_2} \frac{|P - P_0|}{2} \left(\frac{1}{|P_0|} + \frac{1}{|P|} \right) df \tag{5}$$

with f_1 and f_2 being the limiting frequencies of the band analysed. Eq. (5) indicates that the matching between the two results in both amplitude and phase has to be good at all frequencies in order to make the error small. The above definition of error is not the usual one in which case the absolute difference of the erroneous and exact values is divided by the absolute exact value. The usual definition would give an error close to unity if P_0 is much smaller than P , but much larger than unity if vice versa applies.

By using the definition (26) such an anomaly is removed: in both cases the error will be much larger than unity. On the other hand, the error reduces toward zero if the two results converge.

Fig. 4 shows the cumulative error as a function of different cases. The legend below the bar plot indicates graphically the combination of parameters concerned. The tones range from black, indicating the lowest value of the given parameter, towards white, the highest value. N denotes the number of modes. The error is given in dB scale for better visual resolution.

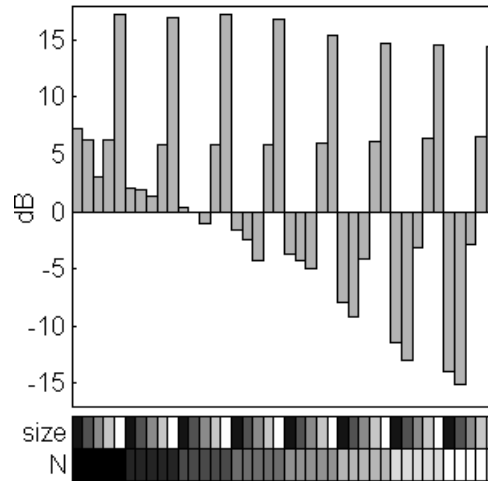


Figure 4 – Cumulative relative error of the coupling method

As expected, the error reduces with the number of modes involved increasing and with the ratio patch size / wavelength decreasing. Very large patch size and small number of modes give always unacceptable results. This applies to all cases where the number of modes is sufficiently high to produce small errors. At lower number of modes the optimum patch size / wavelength ratio is close to 0.3. On the other side, the largest patch size / wavelength ratio gives systematically the largest error, well above unity, which indicates that the two results are of very different magnitude.

If the number of modes is not large enough while the number of patches is large, the conditioning of inverted matrices, Eq. (3) can be poor and lead to considerable errors. Fig. 5 shows the cumulative conditioning number for 40 cases analysed, defined for the sake of convenience as:

$$C_c = \left(\max(C(f)) \cdot \frac{1}{f_2 - f_1} \int_{f_1}^{f_2} C(f) df \right)^{0.5} \quad (6)$$

where $C(f)$ stands for the conditioning number depending on frequency.

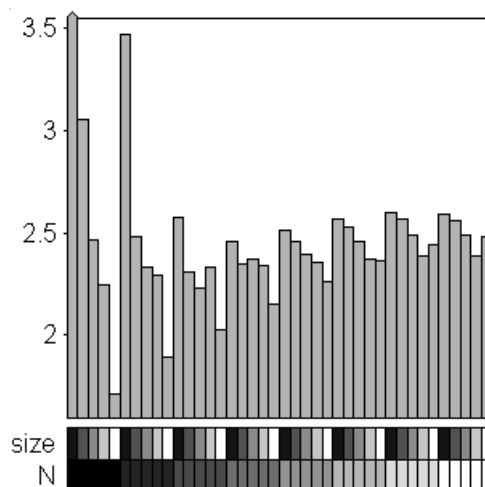


Figure 5 – Log of cumulative conditioning number of test cases. The first column, equal to 18.1, is not fully displayed being considerably larger than the rest of values.

The definition (6) takes into account both the maximum and the mean values of the frequency dependent conditioning number to produce a single value relative to the entire band. In order to account for large variation of C_c values, its logarithm is plotted against different cases. It can be seen that C_c decreases as a rule with the patch size. The lower the number of modes taken into computation the faster the decrease.

3. SOUND IN MULTIPLE CAVITIES USING HARMONIC SURFACE COUPLING

An alternative way to discretized patch surface coupling of acoustical spaces consists in the use of continuous surface functions. The continuous coupling surface technique used decomposes the sound pressure and the particle velocity across a rectangular surface into a number of 2D trigonometric functions q , named surface harmonics. E.g. a rectangular coupling surface of the width b and height h , parallel to the y - z plane of a Cartesian coordinate system will have the function q of order m, n given by the following formula:

$$q_{mn}(y, z) = \phi_y\left(\frac{m\pi y}{b}\right) \cdot \phi_z\left(\frac{n\pi z}{h}\right), \quad m = m_1 \dots M, \quad n = n_1 \dots N \quad (7)$$

For simplicity 2 types of ϕ functions are used, sine and cosine, which produces 2 types of functions q : sin-sin, sin-cos, cos-sin and cos-cos. The values of m_1 and n_1 are equal to 1 for sine and 0 for cosine terms. The entire function basis, limited to integers M and N in the two directions, thus consists of $Q = (2M+1) \times (2N+1)$ space functions q . The selection of appropriate values of M and N depends on the size of the coupling surface, on the acoustical wavelength and field gradients as well as on the desired accuracy.

Two function bases are thus established, one for the sound pressure, one for the normal particle velocity. The two bases can be made equal, which will be the case in this example. With the two bases known, the sound pressure and the particle velocity across the coupling surface are represented in terms of the amplitudes of each surface harmonic q . Again, the frequency-domain representation of variables is used; e.g. the sound pressure is given by $p(y, z, t) = \text{Re}\{P(y, z) \exp(j\omega t)\}$. Expressed in terms of Q surface harmonic amplitudes Π , the y, z – dependent pressure amplitude reads:

$$P(y, z) = \Pi_{00} + \Pi_{01}^{cs} q_{01}^{cs} + \Pi_{10}^{sc} q_{10}^{sc} + \sum_{m=1}^M \sum_{n=1}^N (\Pi_{mn}^{cc} q_{mn}^{cc} + \Pi_{mn}^{cs} q_{mn}^{cs} + \Pi_{mn}^{sc} q_{mn}^{sc} + \Pi_{mn}^{ss} q_{mn}^{ss}) \quad (8)$$

where the superscripts cc, cs etc refer to one of the 4 types of surface harmonic functions q . The normal component of particle velocity at the coupling surface can be represented in an analogous way, by Q complex amplitudes of velocity surface harmonics Γ . The entire set of surface harmonic amplitudes of pressure can be represented by a vector Π of size Q . Likewise, a vector Γ of size Q will accommodate all the velocity surface harmonic amplitudes.

If a unit-amplitude normal velocity excitation, spatially equal to m - n th velocity surface harmonic, is applied to the coupling surface, it will create a sound pressure across this surface which will be in a general case composed of all the pressure surface harmonics. By taking all of Q velocity excitations and computing for each of these all the resultant pressure harmonics, the surface impedance matrix Ω can be found. An arbitrary velocity excitation across the coupling surface, decomposed in surface velocity harmonics represented by the vector of amplitudes Γ , will thus produce the sound pressure across the same surface which, represented by pressure surface harmonics, will have the amplitudes Π that obey $\Pi = \Omega \Gamma$.

The details of the surface harmonic coupling technique, which has been outlined in (4) and further expanded in (5), will be left out for the sake of brevity. The technique will be here used to demonstrate its application to complex acoustical spaces.

3.1 The acoustical space

In the next example the entire acoustical space is composed of 3 parallelepipedic cavities, A, B and C, Fig. 6. The cavities are of 3m height; other dimensions are given in Fig. 6. The cavities are coupled through two rectangular openings S_1 and S_2 of 2m height. A unit point source is located at (2.5, 3.5, 2)m in B. The two openings will act as the coupling interfaces between the 3 cavities. The sound pressure will be computed across two plane surfaces indicated by dashed lines, one in A the other in C. The computation will be done by Actran software since the validation of the results obtained by coupling of the three rooms could not be done analytically.

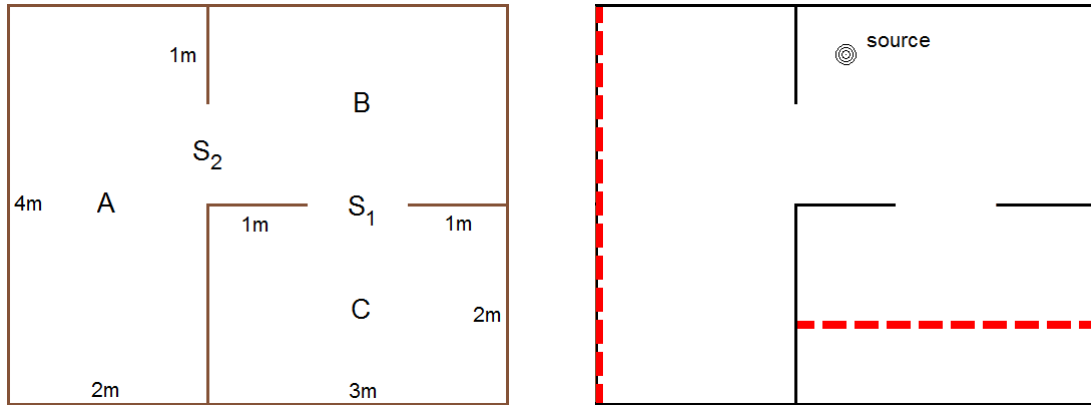


Figure 6 – The acoustical space. Left: geometry; right: source and response positions.

Figure 7 shows the space-averaged RMS sound pressure across the two response surfaces. The modal density is high, increasing with frequency which is a characteristic feature of closed spaces.

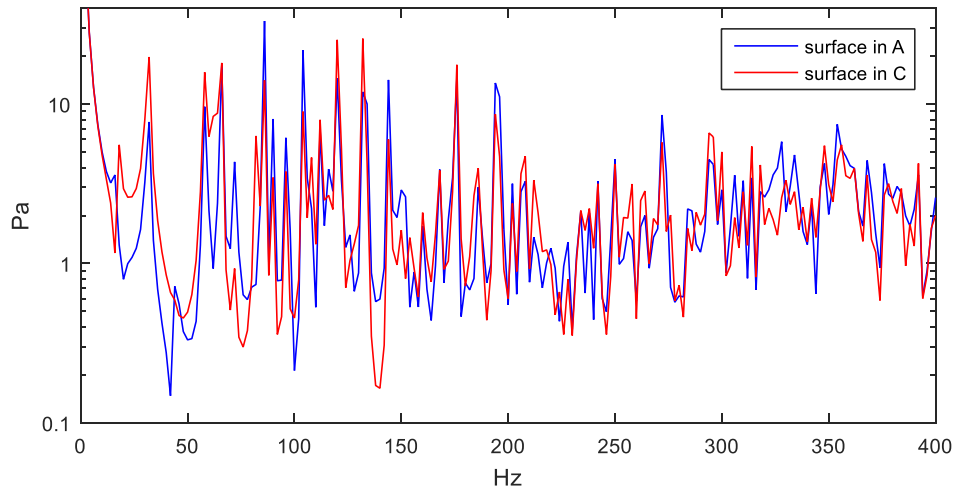


Figure 7 – RMS spectra of space-averaged sound pressure.

The next two figures show the difference of space-averaged levels obtained by direct computation and by the coupling technique. Two different numbers of harmonics per coupling surface were applied: $Q = 15$ ($M=2, N=1$) and $Q = 45$ ($M=4, N=2$). Fig. 8 refers to the space A, the next one to the space C.

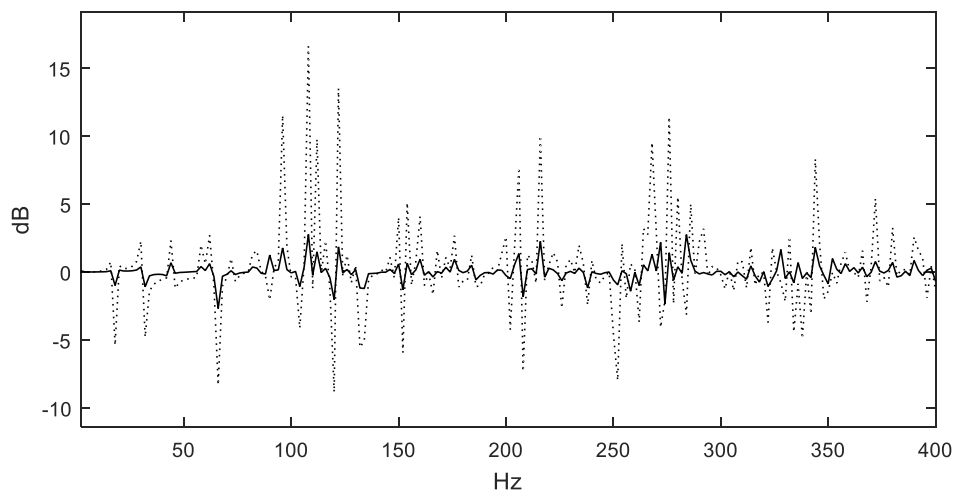


Figure 8 – Level difference of space-averaged spectra across the response surface in A by direct and coupling methods. Full line: 45 harmonics; dotted line: 15 harmonics.

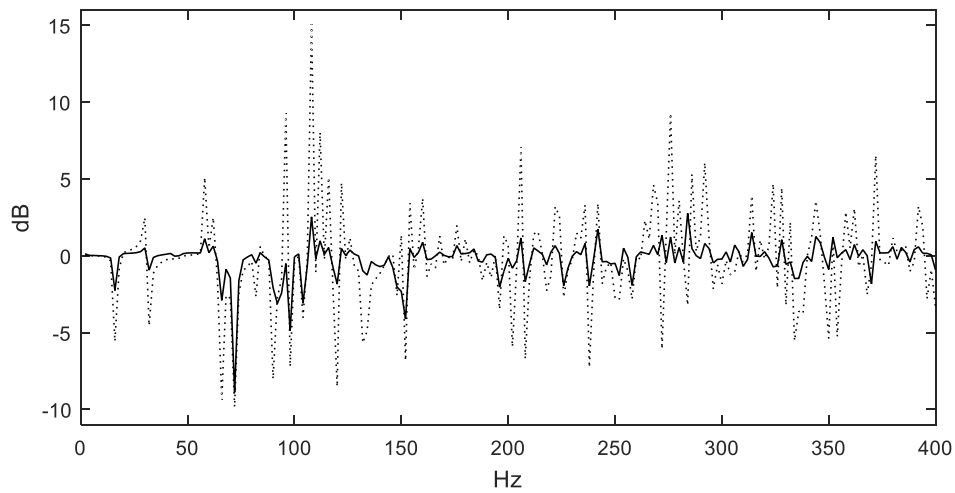


Figure 9 – Level difference of space-averaged spectra across the response surface in C by direct and coupling methods. Full line: 45 harmonics; dotted line: 15 harmonics.

One can see that the use of 15 harmonics only yields fairly large discrepancies with the reference result at some frequencies. Using 3 times larger number of harmonics gives much better matching.

The next two figures shows the instantaneous pressure across the response surface in the space A at two different frequencies. Again, the use of larger number of harmonics provides more accurate result.

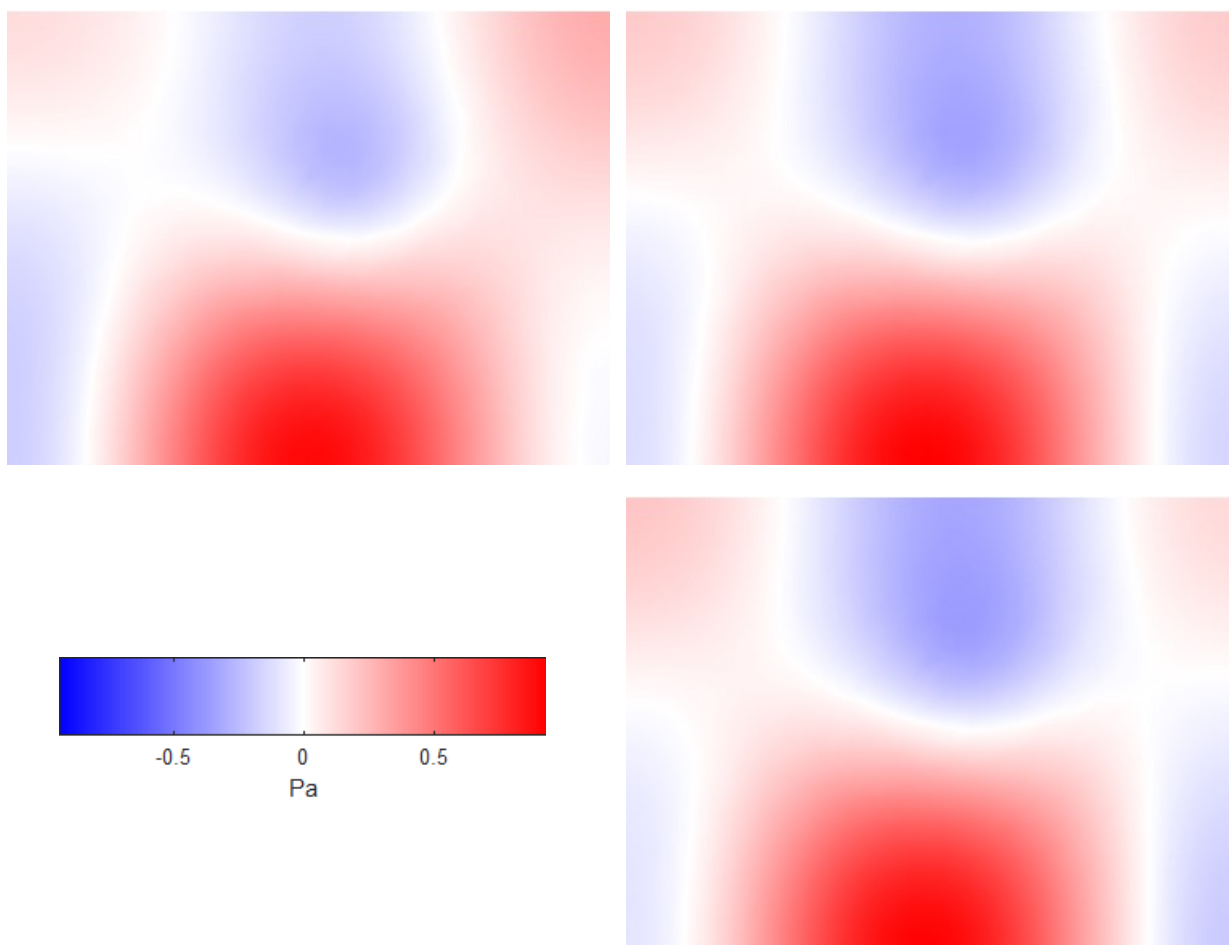


Figure 10 – Instantaneous sound pressure across the response surface in A at 100 Hz. Top left: 15 harmonics; top right: 45 harmonics, bottom: reference value.

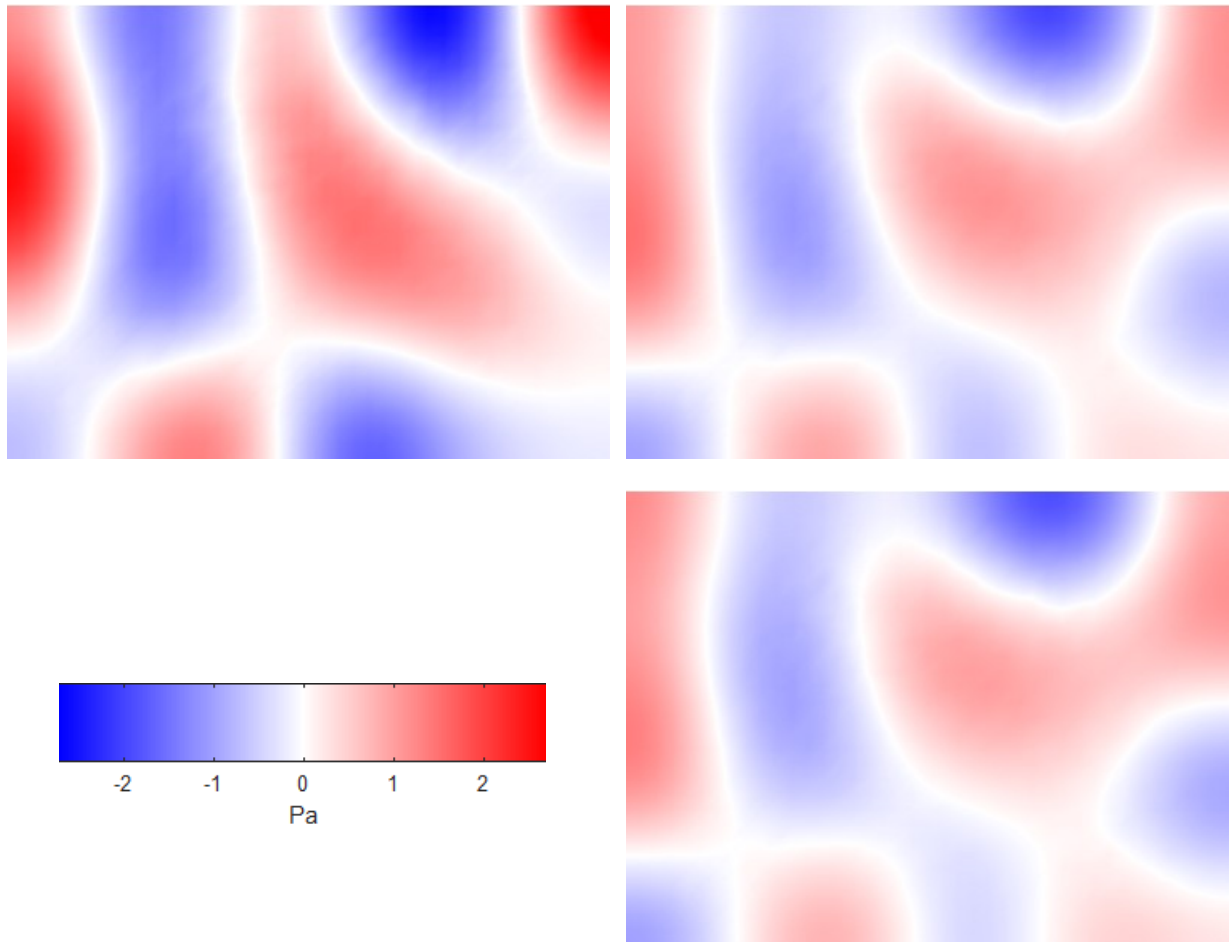


Figure 11 – Instantaneous sound pressure across the response surface in A at 200 Hz. Top left: 15 harmonics; top right: 45 harmonics, bottom: reference value.

4. CONCLUSIONS

Using simple examples it is shown how the surface coupling of simple acoustical spaces can be applied to obtain the sound response in a complex space. The modelling by coupling can be done using analytical models of simple spaces. Two techniques applied, the patch and the surface harmonic technique, are shown to produce acceptable results.

ACKNOWLEDGEMENTS

The research of Mrs Du was supported by the China Scholarship Council. The Laboratory of Vibration and Acoustics - INSA Lyon is member of CeLyA acoustics organization.

REFERENCES

1. Hodgson M, Bradley J. Sound in Rooms. In: Ver IL, Beranek LL, editors. Noise and Vibration Control Engineering - Principles and Applications. 2nd ed. New York, USA: Wiley; 2006. p. 181-214.
2. Hong WK, Kim J, Natural mode analysis of hollow and annular elliptical cylindrical cavities, J Sound Vib. 1995;183(2):327–351.
3. Abom M, Derivation of four-pole parameters including higher order mode effects for expansion chamber mufflers with extended inlet and outlet, J Sound Vib. 1990;137 (2): 403–418.
4. Pavic G, Air-borne sound source characterisation by plane surface harmonics. Proc INTER-NOISE 2012, August 19-22 2012, New York, USA
5. Du L, Characterisation of Air-borne Sound Sources using Surface Coupling Techniques, PhD Thesis, 2016, University of Lyon, France.

